Metabolic reprogramming identifies the most aggressive lesions at early phases of hepatic carcinogenesis

SUPPLEMENTARY FIGURES AND TABLE

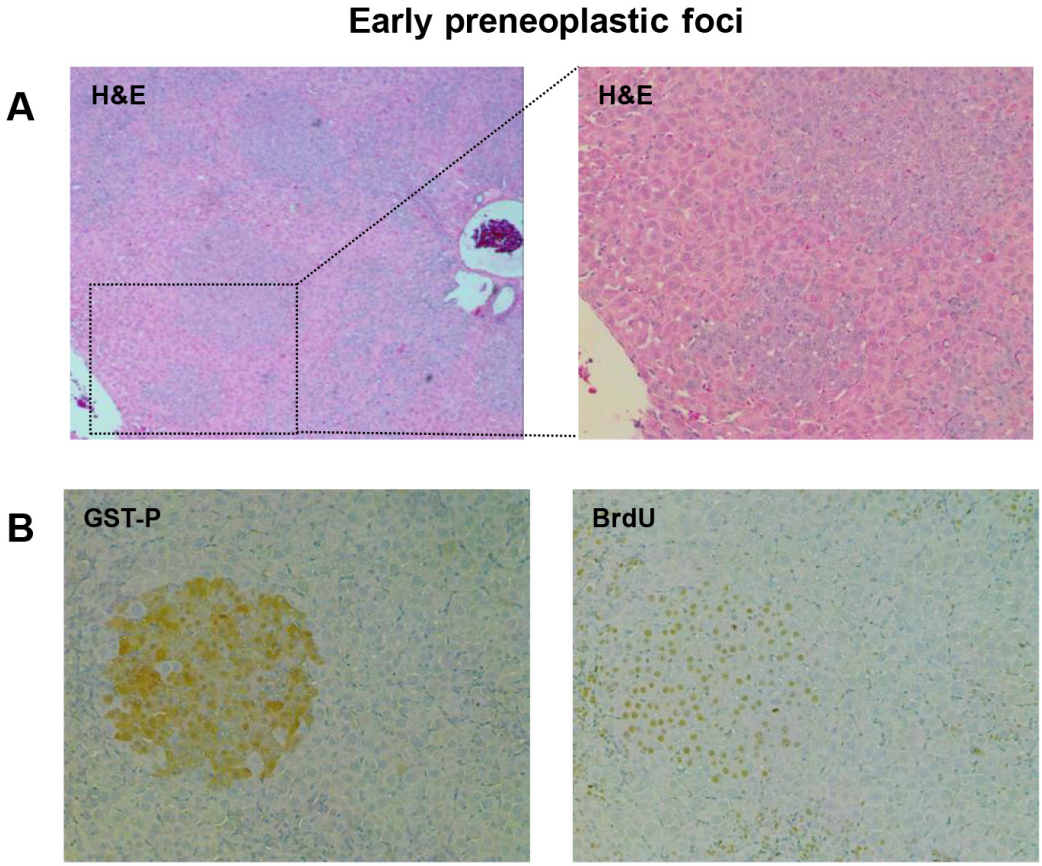

Supplementary Figure S1: Strong proliferative activity in early preneoplastic foci. A. H&E staining of basophilic foci developed 1 week after PH (x4). Inset: higher enlargement (x10). **B.** Microphotograph showing that most of nuclei are stained for BrdU (right) in a GSTP+ EPFs (x10). Several mitoses are present. BrdU was given in drinking water for 24 hours prior to sacrifice.

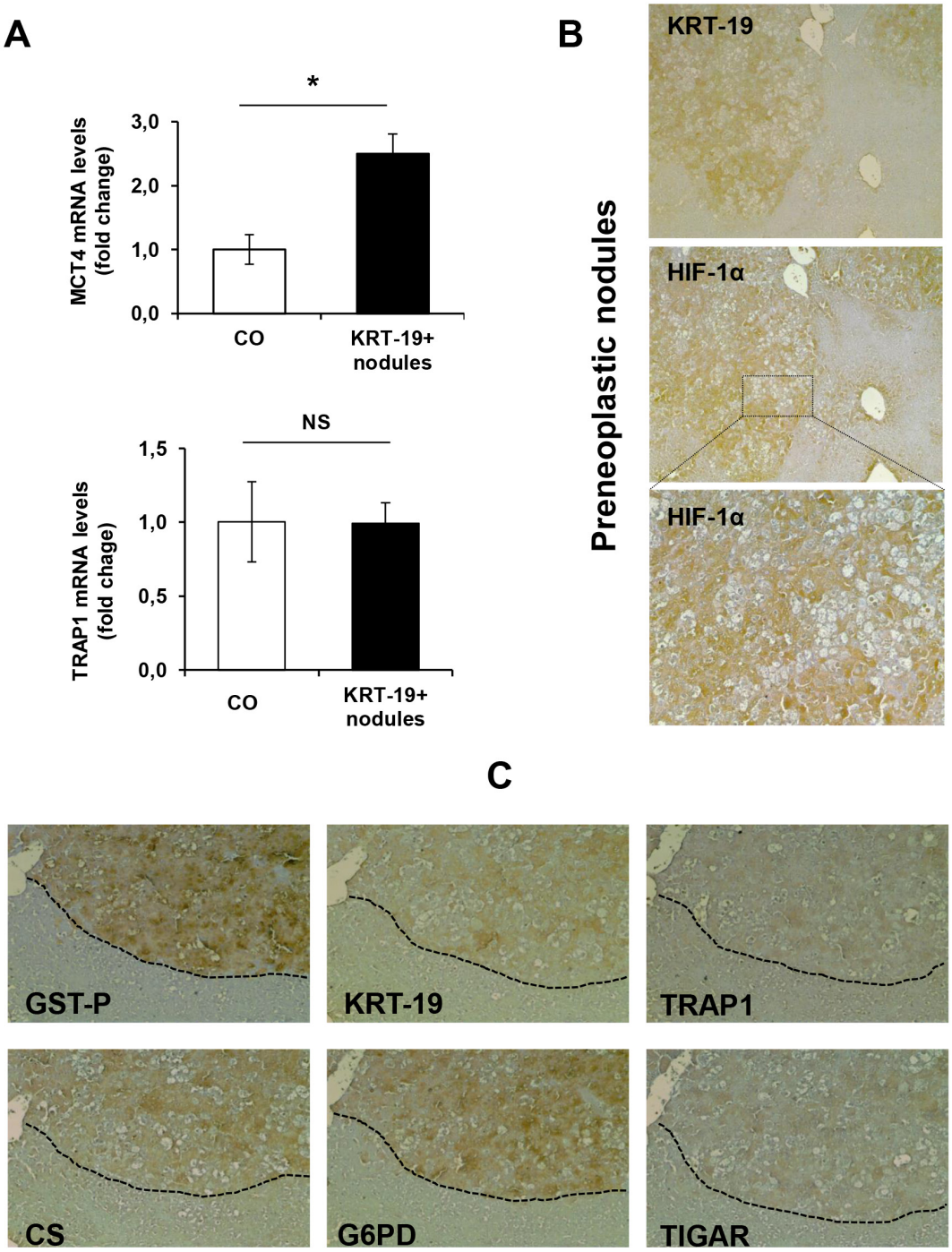

Supplementary Figure S2: Analysis of markers of metabolic change in preneoplastic nodules. A. qRT-PCR analysis of MCT4 and TRAP1 in laser-microdissected GST-P$^+$ preneoplastic nodules. Gene expression is reported as fold-change relative to age-matched controls; *P<0.05, NS: not significant. **B.** Strong HIF-1α expression in a KRT-19$^+$ nodule (x4). Inset: enlargement showing nuclear HIF-1α staining (x10). **C.** IHC analysis on serial sections of liver nodules showing an heterogeneous staining for TRAP1, CS and TIGAR in GST-P$^+$/KRT-19+ nodules (x20).

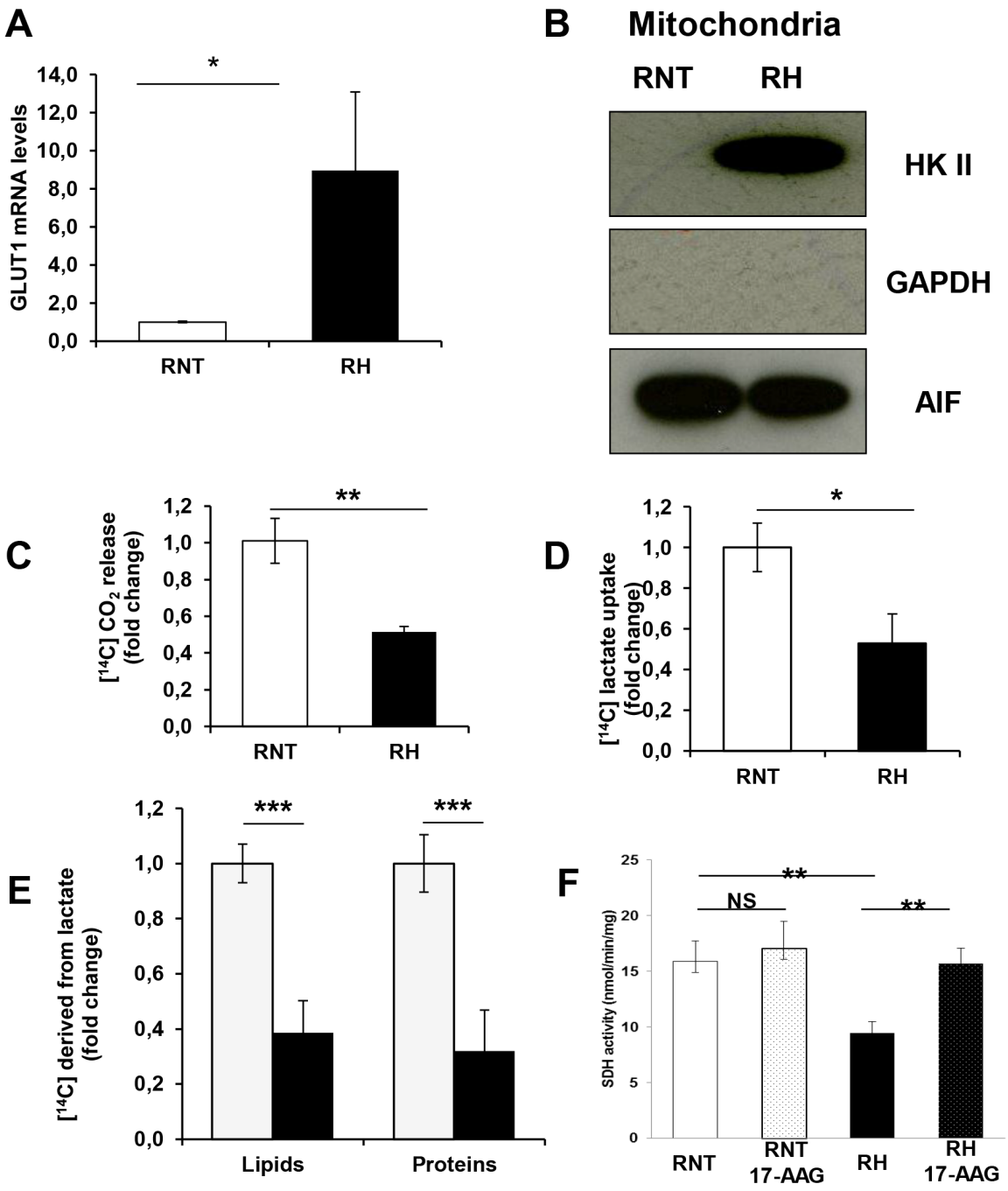

Supplementary Figure S3: RH cells display a higher glucose metabolism and a lower SDH activity than RNT cells. **A.** qRT-PCR analysis of GLUT1 mRNA levels in RNT and RH cells. Values are reported as fold-change relative to RNT cells; **P*<0.05. **B.** Western immunoblots analysis of HK II expression on mitochondrial fractions of HCC derived cells (RH) and of the non-tumorigenic hepatocytes (RNT). Blots were probed with anti-AIF and anti-GAPDH antibodies to check for mitochondrial protein load and cytosolic contaminants, respectively. **C.** Radioactive assays using [^{14}C]-glucose revealed an impairment of total CO_2 production (*i.e.* OXPHOS) in RH cells. **D.** Lactate uptake in RNT and RH cells; **P*<0.05**. E.** Radioactive signal derived from lipids and proteins obtained from [^{14}C] lactate in RNT and RH cells; ****P*<0.001. **F.** Analysis of the SQR enzymatic activity of SDH in RNT and RH cells; when indicated, cells were treated with the TRAP1 inhibitor 17-AAG (5 μM).

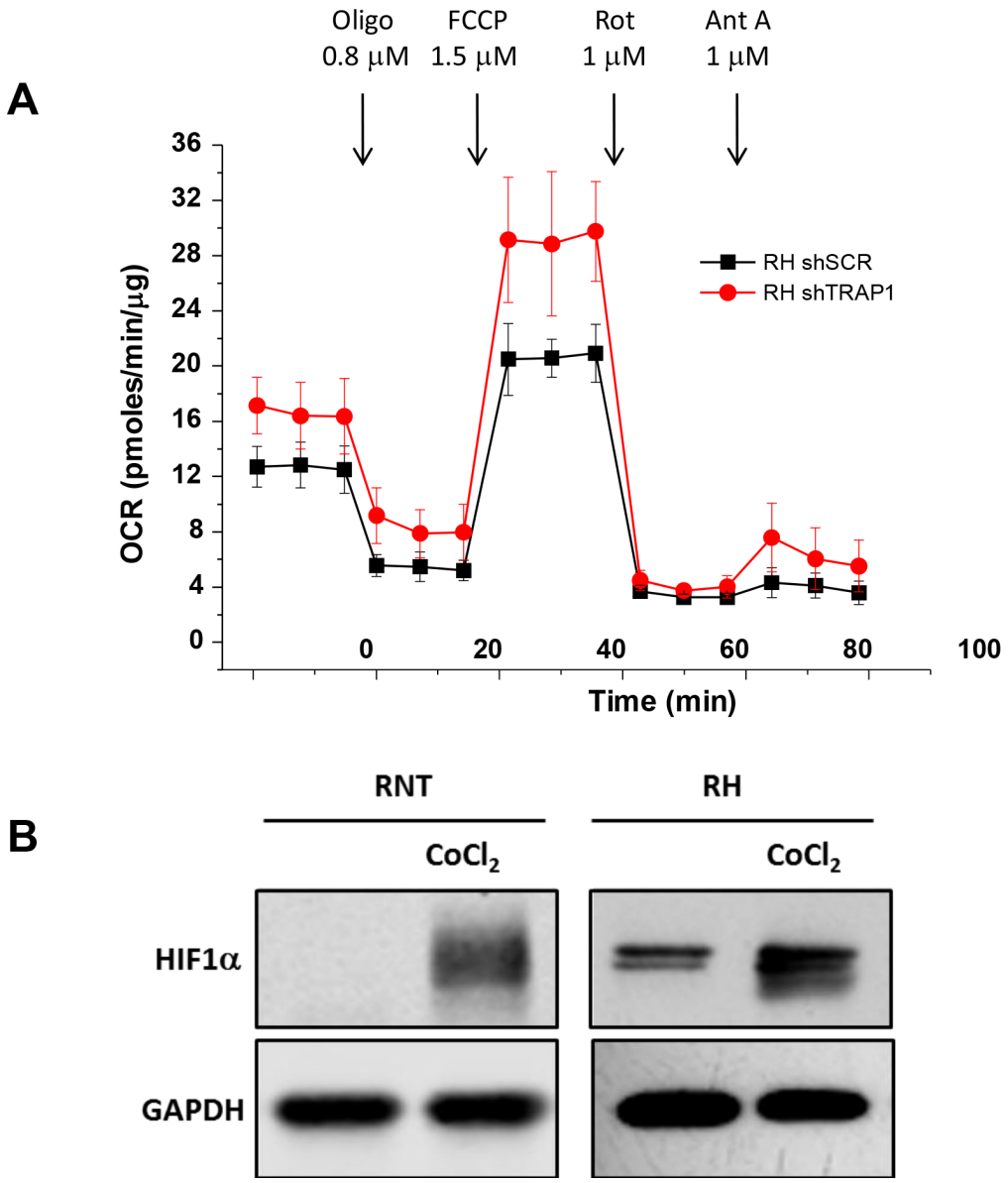

Supplementary Figure S4: A. Measurements of oxygen consumption rate (OCR, right) on TRAP1-silenced RH cells. Addition of oligomycin, FCCP, rotenone, and antimycin A was carried out at the indicated times. **B.** WB showing lack of HIF-1α in RNT cells. $CoCl_2$ (200 µM, 6 hours) is used as a positive control for HIF-1α stabilization.

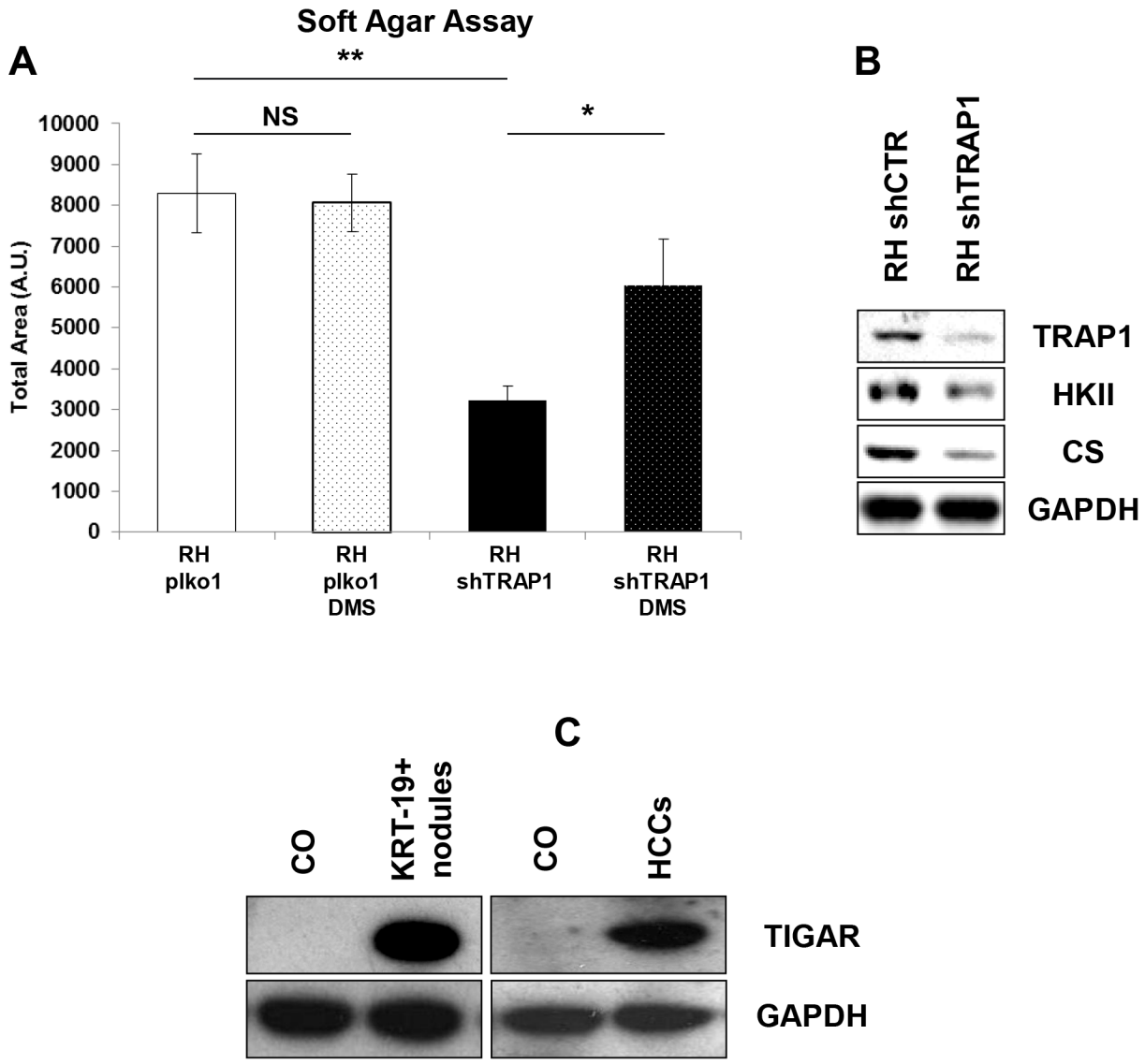

Supplementary Figure S5: Knocking-down TRAP1 expression inhibits tumorigenicity and the expression of metabolic enzymes in RH cells. A. Soft agar tumorigenesis assays were performed in RH cells following TRAP1 silencing and in combination with di-methyl-succinate (DMS, 5 mM) treatment. Data indicate the total colony area at the 25th experimental day. **B.** Western immunoblots showing TRAP1, HK II and CS expression on extracts from RH cells following TRAP1 silencing. GAPDH was used as a loading control. **C.** Western immunoblots showing increased TIGAR expression in KRT-19^{+} nodules and HCC samples compared to control liver (CO). GAPDH was used as a loading control.

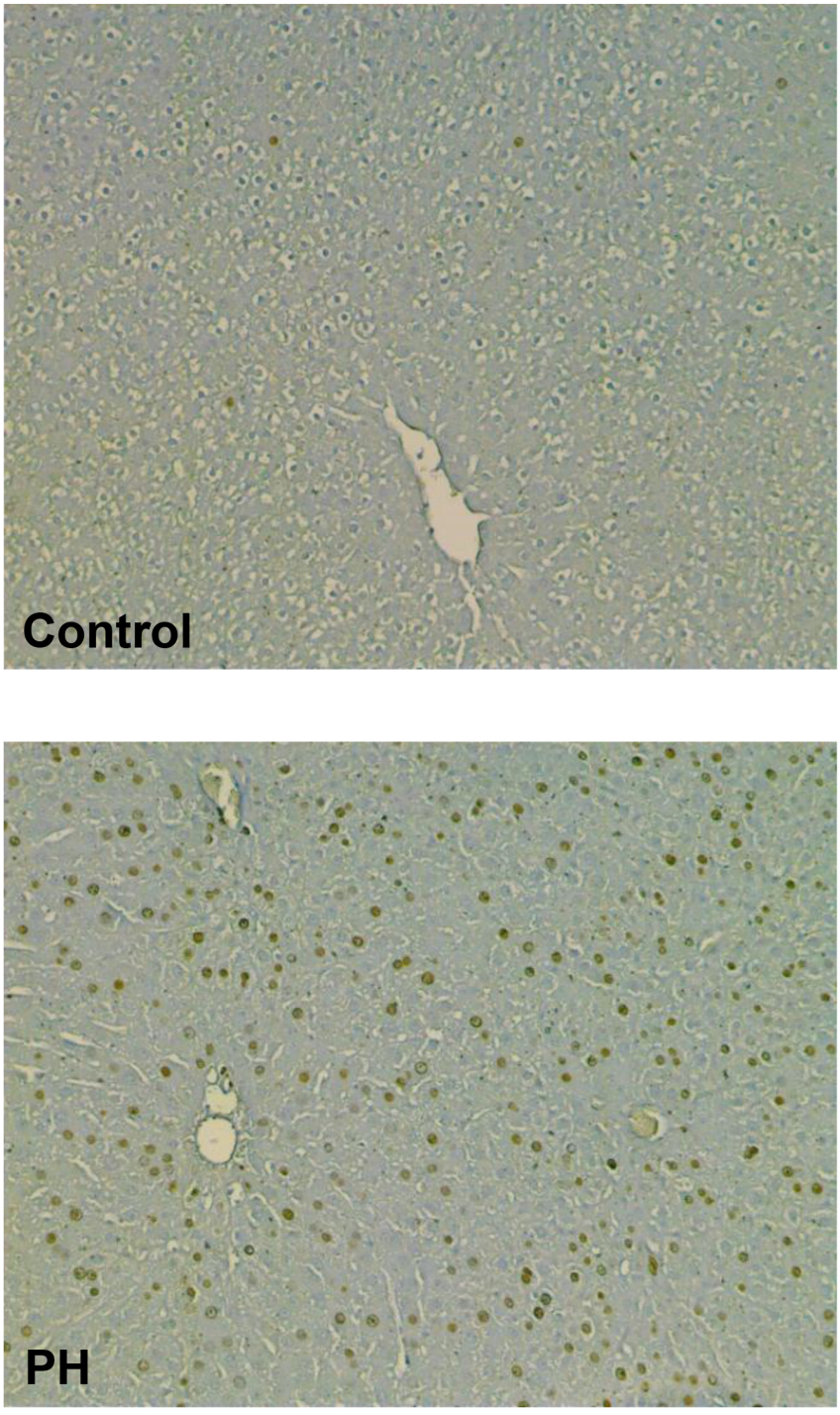

Supplementary Figure S6: BrdU incorporation in hepatocyte nuclei 24 hours after 2/3 partial hepatectomy (PH). Microphotograph showing BrdU staining of hepatocyte nuclei (x10). BrdU (100 mg/kg) was given intraperitoneally to animals subjected to surgery and to controls 2 hours prior to sacrifice.

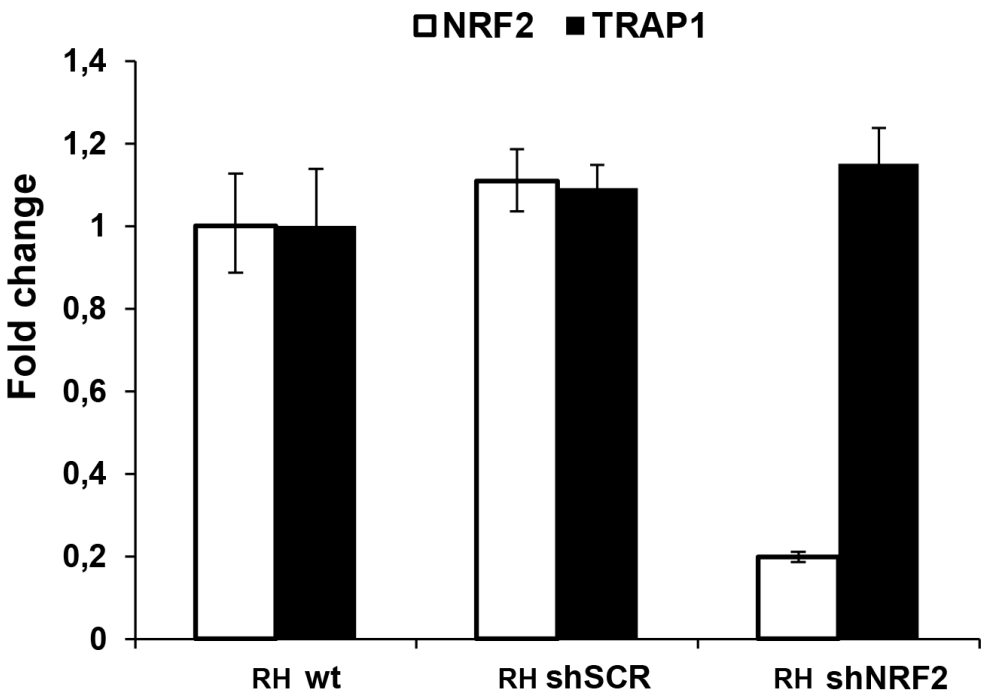

Supplementary Figure S7: qRT-PCR analysis of NRF2 and TRAP1 mRNA levels in RH cells upon NRF2 silencing. Values are reported as fold-change relative to cells untransduced wt cells.

A

GENE SYMBOL	FOLD INDUCTION KRT-19+ nodules
G6PD	5.77
miR-1	-5.20

B

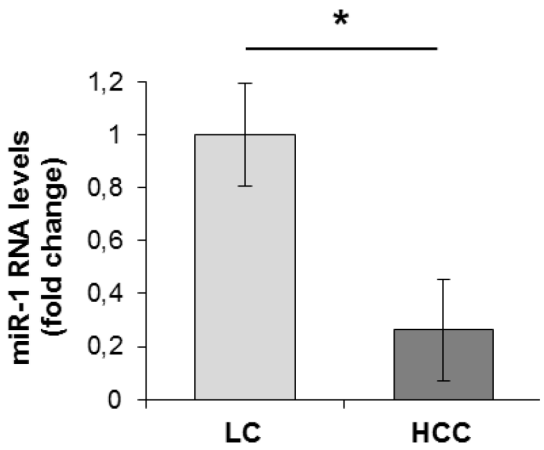

C

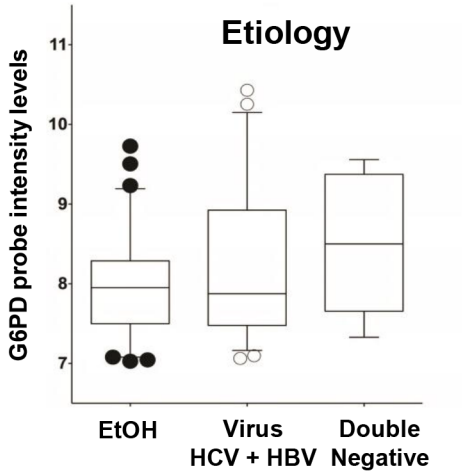

Supplementary Figure S8: G6PD induction in early preneoplastic lesions and human HCC. A. Illumina microarray (RatRef-12 V1) and TaqMan Low Density Arrays were used to determine G6PD and miR-1 expression, respectively, in KRT-19^{+} nodules 10 weeks after treatment with DENA. **B.** Changes in miR-1 and G6PD levels in human HCCs. QRT-PCR analysis of miR-1 expression in human resected HCCs (n=59) and their peritumoural cirrhotic liver (Liver cirrhosis, LC; n=59). miR-1 expression is calculated as fold change difference compared to LC. Error bars represent SEM; U6RNA was used as endogenous control; *P< 0.05. **C.** Stratification of patients according to their etiology did not reveal any significant association with G6PD levels.

Supplementary Table S1: Study population characteristics.

See Supplementary File 1